

Locality and thermalization in closed quantum systems

J. Sirker, N. P. Konstantinidis, and N. Sedlmayr

Department of Physics and Research Center OPTIMAS,
Technical University Kaiserslautern, D-67663 Kaiserslautern, Germany

(Dated: December 2, 2024)

We study the non-equilibrium dynamics of observables for finite one-dimensional quantum systems. By calculating the dependence of time and statistical averages on system size we investigate the role of the local and the exponentially many non-local conserved quantities for thermalization. We derive, in particular, a Mazur-type equality to split observables into a local and a non-local part. For an initial state distribution which is not narrow in energy, so that the eigenstate thermalization hypothesis cannot hold, we then demonstrate that oscillations in the non-local part are, in general, responsible for thermalization while the time and statistical ensemble averages for the local part are identical due to energy conservation.

PACS numbers: 05.30.Ch, 05.70.Ln, 75.10.Pq

Introduction Starting a classical many-body system from a *typical* initial configuration we expect that the system equilibrates at long times so that *typical* observables become time independent. Relevant scenarios include, for example: (I) Particles confined in a box with a given smooth velocity distribution where at time t_0 a valve is opened so that they can expand into a larger space. (II) Two spatially separated sets of particles with smooth velocity distributions having different mean values where at time t_0 a valve is opened so that they can mix.

If the ensuing dynamics is ergodic, then the *ergodic theorem* [1–4] tells us that we can replace the time average of typical observables by an ensemble average. The ensemble provides a probability measure ρ on phase space which has to be invariant under time evolution because it describes the stationary state reached after the system has thermalized. The probability measure thus has to be a function of the conserved quantities \mathcal{Q}_j with $\{\mathcal{H}, \mathcal{Q}_j\} = 0$ where $\{.,.\}$ is the Poisson bracket and \mathcal{H} the Hamilton function of the system. In cases where \mathcal{H} is the only independent conserved quantity this invariant phase space measure is the familiar microcanonical ensemble which becomes equivalent to the canonical one in the thermodynamic limit (TDL). Integrable systems with phase space dimension $2N$, on the other hand, have N independent conservation laws making them non-ergodic and restricting the motion in phase space to invariant tori. Importantly, the Kolmogorov-Arnold-Moser (KAM) theorem allows us to describe the consequences of small integrability breaking perturbations on a quantitative level [4, 5].

Although recent theoretical [6–11] and experimental [12–15] studies have lead to new interesting insights, it is still fair to say that the non-equilibrium dynamics of a quantum system is much less well understood. One example, which has been studied numerically [8], is the expansion of a bosonic lattice gas into a larger empty lattice. This is reminiscent of the classical case above (I) with an energy distribution function for the initial

state which is singly peaked [8]. Another case which has been intensively studied are quantum quenches in lattice models with short-range interactions [9, 16–24]. This typically also seems to lead to a *singly-peaked* initial energy distribution. Thermalization in such cases has often been attributed to the observation that the eigenstate expectation values of the specific considered observable fluctuate little between eigenstates close in energy and can be directly replaced by an ensemble average, a concept dubbed *eigenstate thermalization hypothesis* (ETH) [6–8, 25].

The class of problems we expect thermalization for is, however, much broader [26]. In particular, thermalization should also occur for the quantum analogue of case (II): an initial energy distribution which is peaked at two distinct energies. It is exactly this more generic case which we want to investigate in this letter.

We want to restrict our discussion to time-independent Hamiltonians H which have short-range interactions in position space and a discrete spectrum [44]. The time average of an observable O for an initial pure state $|\Psi_0\rangle$ is defined by

$$\bar{O} = \lim_{\tau \rightarrow \infty} \frac{1}{\tau} \int_0^\tau dt \langle \Psi_0 | e^{iHt} O e^{-iHt} | \Psi_0 \rangle. \quad (1)$$

By using a spectral representation of the observable O and assuming that the spectrum of H is non-degenerate we immediately obtain

$$\bar{O} = \langle O \rangle_{\text{diag}} \equiv \langle \Psi_0 | O_{\text{diag}} | \Psi_0 \rangle = \sum_n O_{nn} \underbrace{|\langle \Psi_0 | n \rangle|^2}_{|c(n)|^2} \quad (2)$$

where $O_{\text{diag}} = \sum_n O_{nn} P_n$. Here $O_{nn} = \langle n | O | n \rangle$ with $P_n = |n\rangle\langle n|$ being the projection operator onto the eigenstate $|n\rangle$ and $H|n\rangle = \varepsilon_n|n\rangle$. In the case of degeneracies, Eq. (2) remains valid if we choose the energy eigenbasis in which O is diagonal in the degenerate subspaces.

If we want to replace the time average by an ensemble average following the prescription in the classical case,

we immediately encounter an important aspect which is different from the classical problem: All the projection operators are conserved, $[H, P_n] = 0$, and the number of conserved quantities thus always equals the Hilbert space dimension D . A density matrix ρ_{diag} which yields a statistical average equal to the time average (2) thus apparently has to be a function of all the projection operators [26], e.g.,

$$\rho_{\text{diag}} = \exp\left(-\sum_n \lambda_n P_n\right) / Z_{\text{diag}} \quad (3)$$

with $Z_{\text{diag}} = \text{Tr} \rho_{\text{diag}}$ and Lagrange multipliers λ_n fulfilling the condition $e^{-\lambda_n} / Z_{\text{diag}} = |\langle \Psi_0 | n \rangle|^2$. While this ensemble fulfills $\text{Tr}(O \rho_{\text{diag}}) = \langle O \rangle_{\text{diag}} \equiv \bar{O}$, see Eq.(2), by construction and thus naively proves the ergodic theorem in the quantum case, it depends on the initial state and completely fixes the *microstate*. In quantum statistical mechanics we are, however, only interested in the *macrostate* consisting of many microstates which cannot be distinguished by local probes [26].

The new important ingredient, which has to be taken into account in the quantum case, is the distinction between *local* and *non-local* conserved quantities. A local operator for a lattice model is defined as $\mathcal{Q}_m = \sum_j q_j^m$ where q_j^m acts on lattice sites $j, j+1, \dots, j+m$ only, with m finite. In a field theory this then becomes a fully local operator $\mathcal{Q}_m = \int d\mathbf{r} q^m(\mathbf{r})$. In the TDL we expect that only the local conserved quantities are needed in the density matrix to describe the thermalized state. This number is usually finite for a generic quantum system while it increases linearly—but not exponentially!—with system size for an integrable one-dimensional model [27, 28]. Experiments on cold atomic gases as well as most numerical studies of the thermalization problem are, however, done on finite systems [8, 19, 29] where a distinction between local and non-local conservation laws, strictly speaking, does not exist. Understanding the scaling of local and non-local contributions with system size is therefore a problem of practical relevance.

General considerations: A Mazur-type equality If we want to study thermalization on the microscopic level of individual eigenstates we can write

$$\begin{aligned} 0 &= \lim_{N \rightarrow \infty} \Delta O_N \equiv \lim_{N \rightarrow \infty} [\langle O \rangle_{\text{diag}} - \langle O \rangle_{\text{th}}] \quad (4) \\ &= \lim_{N \rightarrow \infty} \sum_{n=1}^D \underbrace{\frac{\langle O P_n \rangle_{\text{th}}}{\langle P_n^2 \rangle_{\text{th}}}}_{O_{nn}} \left(\underbrace{\langle \Psi_0 | P_n | \Psi_0 \rangle}_{|c(n)|^2} - \underbrace{\langle P_n \rangle_{\text{th}}}_{\rho_{\text{th}}^{nn}} \right) \\ &\stackrel{N \rightarrow \infty}{\rightarrow} \int d\varepsilon O(\varepsilon) \left[\underbrace{|\langle c(\varepsilon) \rangle|^2 \nu(\varepsilon)}_{\Gamma_{\text{diag}}(\varepsilon)} - \underbrace{\rho_{\text{th}}(\varepsilon) \nu(\varepsilon)}_{\Gamma_{\text{th}}(\varepsilon)} \right] \end{aligned}$$

where $\langle O \rangle_{\text{th}} = \text{Tr}\{O \rho_{\text{th}}\}$ with $\rho_{\text{th}} = \exp(-\sum_j \lambda_j \mathcal{Q}_j) / Z$, $Z = \text{Tr} \rho_{\text{th}}$ being the appropriate thermal density matrix including all the local conserved quantities \mathcal{Q}_j with $\{\lambda_j\}$ determined by $\langle \Psi_0 | \mathcal{Q}_j | \Psi_0 \rangle = \text{Tr}\{\mathcal{Q}_j \rho_{\text{th}}\}$ [21]. The

thermal energy distribution $\Gamma_{\text{th}}(\varepsilon)$ includes the density of states $\nu(\varepsilon)$ and becomes sharply peaked at one specific energy in the TDL. We can now ask why Eq. (4) vanishes. Is it (a) because the two distribution functions $\Gamma_{\text{diag}}(\varepsilon)$ and $\Gamma_{\text{th}}(\varepsilon)$ approach each other implying thermalization for *any* observable O or is it (b) due to fluctuations in O_{nn} ? In cases analogue to the classical setup (I) as considered in [8], point (a) can be part of the explanation, however, for a generic initial distribution $|c(n)|^2$ this cannot be the case. To investigate scenario (b), which has to be the explanation in the general case, we continue by explaining how to separate O_{nn} into a local and a non-local part.

The distinction between local and non-local conserved quantities is also essential for quantum transport. Here it is known that a local or quasi-local [30] conserved quantity can protect a current from decaying while a non-local conserved quantity cannot [31–34]. This is understood by using a Mazur equality [31, 35, 36] where the current operator is written as a sum of projections onto all the conserved quantities of the system. In exactly the same way, we can project the considered observable onto the local and non-local conserved quantities to study thermalization. We first assume that the system has only a single local conservation law—the Hamiltonian itself—and generalize to the case of several local conservation laws later. Then we expect that the canonical ensemble $\rho_{\text{th}} = \exp(-H/T) / Z$ describes the system at long times in the TDL [45]. As in Eq. (4) we can write $O_{nn} = \langle O P_n \rangle_{\text{th}} / \langle P_n^2 \rangle_{\text{th}}$ with $\langle P_n P_m \rangle_{\text{th}} = \delta_{nm} \langle P_n^2 \rangle_{\text{th}}$ [46]. The Hamiltonian itself can be written as $H = \sum_n \varepsilon_n P_n$. By constructing the $(D-1)$ many orthogonal linear combinations \bar{P}_n [47] we can split O_{diag} into a local and a non-local part

$$O_{\text{diag}} = \underbrace{\frac{\langle O H \rangle_{\text{th}}}{\langle H^2 \rangle_{\text{th}}}}_{O_{\text{loc}}} H + \underbrace{\sum_{n=1}^{D-1} \frac{\langle O \bar{P}_n \rangle_{\text{th}}}{\langle \bar{P}_n^2 \rangle_{\text{th}}}}_{O_{\text{nonloc}}} \bar{P}_n \quad (5)$$

with $\langle H \bar{P}_n \rangle_{\text{th}} = 0$ and $\langle \bar{P}_n \bar{P}_m \rangle_{\text{th}} = \delta_{nm} \langle \bar{P}_n^2 \rangle_{\text{th}}$. Energy conservation demands $\langle \Psi_0 | H | \Psi_0 \rangle = \langle H \rangle_{\text{th}}$ which fixes the temperature T [8, 10, 17] and guarantees the equivalence of the diagonal and canonical ensemble average for the first term in (5). Eq. (4) can thus be rewritten as a condition for the non-local part only.

We are typically interested in observables O which are not affected by an energy shift $H' = H - E_0$. In this case we can simplify the condition on the non-local part further by demanding that $\langle O_{\text{nonloc}} \rangle_{\text{th}} = 0$. For this gauge we have to choose the reference energy

$$E_0 = \frac{\langle O H \rangle_{\text{th}} \langle H \rangle_{\text{th}} - \langle O \rangle_{\text{th}} \langle H^2 \rangle_{\text{th}}}{\langle O H \rangle_{\text{th}} - \langle O \rangle_{\text{th}} \langle H \rangle_{\text{th}}} \quad (6)$$

The condition for thermalization (4) then reads

$$\begin{aligned}
0 &= \lim_{N \rightarrow \infty} \langle O_{\text{nonloc}} \rangle_{\text{diag}} = \lim_{N \rightarrow \infty} \underbrace{\sum_{n=1}^{D-1} \Delta \bar{O}_N(n)}_{\Delta O_N} \\
&\equiv \lim_{N \rightarrow \infty} \underbrace{\sum_{n=1}^{D-1} \frac{\langle O \bar{P}_n \rangle_{\text{th}}}{\langle \bar{P}_n^2 \rangle_{\text{th}}}}_{\bar{O}_{nn}} \langle \Psi_0 | \bar{P}_n | \Psi_0 \rangle. \quad (7)
\end{aligned}$$

We emphasise that ΔO_N does not depend on the energy shift E_0 nor on the choice of the inner product. If thermalization to the canonical ensemble does occur, then Eq. (7) has to be true for all typical operators O and typical initial states $|\Psi_0\rangle$. For a system which has other local conserved quantities \mathcal{Q}_j apart from H , we can generalize (5) by replacing $O_{\text{loc}} = \sum_j \frac{\langle O \mathcal{Q}_j \rangle}{\langle \mathcal{Q}_j^2 \rangle} \mathcal{Q}_j$.

The model So far, our discussion has been general. To test the concepts we have introduced above, we want to study in the following a specific lattice model, the one-dimensional anisotropic Heisenberg model

$$\begin{aligned}
H(\Delta, J_2) &= J \sum_{j=1}^N h_{j,j+1} + J_2 \sum_{j=1}^N h_{j,j+2}, \quad (8) \\
h_{i,j} &= \frac{1}{2} (S_i^+ S_j^- + h.c.) + \Delta S_i^z S_j^z,
\end{aligned}$$

where S is a spin-1/2 operator, J (J_2) are the superexchange couplings for the nearest (next-nearest) neighbors, respectively, and Δ parametrizes an exchange anisotropy. In the following we set $J = 1$, use periodic boundary conditions, and study the model by exact diagonalization taking spin and spatial symmetries into account [37]. The model (8) is integrable for $J_2 = 0$. In this case the number of conserved local operators \mathcal{Q}_j increases linearly with system size N . In the non-integrable case $J_2 \neq 0$, H itself and $S_{\text{tot}}^z = \sum_j S_j^z$ are the only conserved local operators. To make contact with previous thermalization studies, we first consider a quench scenario [38, 39]. As initial state we choose the ground state $|\Psi_0(\Delta, J_2)\rangle$ of the Hamiltonian (8) with parameters Δ and J_2 . We then time evolve with $H(\bar{\Delta}, \bar{J}_2)$ where $(\bar{\Delta}, \bar{J}_2) \neq (\Delta, J_2)$.

Locality and statistical ensemble We start by studying the role played by non-local conserved quantities for the statistical ensemble. To do so we compare an extended ensemble

$$\rho_{\bar{P}_n} = \exp(-\beta H + \lambda_n \bar{P}_n) / Z, \quad (9)$$

where the parameters β, λ_n are determined by $\langle \Psi_0 | H | \Psi_0 \rangle = \text{Tr}\{H \rho_{\bar{P}_n}\}$ and $\langle \Psi_0 | \bar{P}_n | \Psi_0 \rangle = \text{Tr}\{\bar{P}_n \rho_{\bar{P}_n}\}$, with the canonical and the diagonal ensemble in Fig. 1. The results for the finite size scaling are consistent with the following: (1) The change in the average of an observable caused by including an additional non-local conservation law vanishes exponentially with system size. (2) The contribution of all non-local conservation quantities to the ensemble average vanishes linearly in $1/N$. This

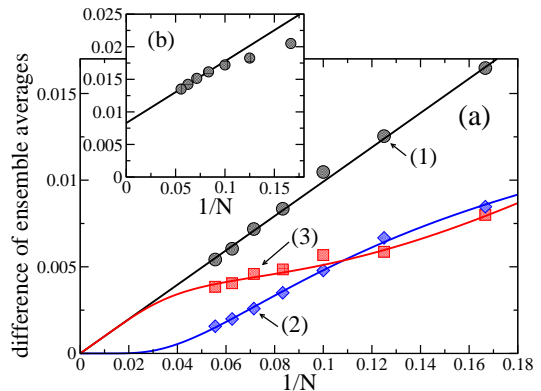


FIG. 1: (Color online) (a) Quench with $|\Psi_0(5, 0.2)\rangle$ and $H(1, 0.2)$. Expectation values $\langle \mathbf{S}_i \mathbf{S}_{i+1} \rangle$ using different ensembles: (1) Difference between canonical and diagonal ensemble and linear fit, (2) between canonical and extended ensemble $\rho_{\bar{P}_1}$ and exponential fit, (3) between $\rho_{\bar{P}_1}$ and the diagonal ensemble and the difference of the two fits. (b) Difference of canonical and diagonal ensemble average for an integrable quench with $|\Psi_0(5, 0)\rangle$ and $H(1/2, 0)$.

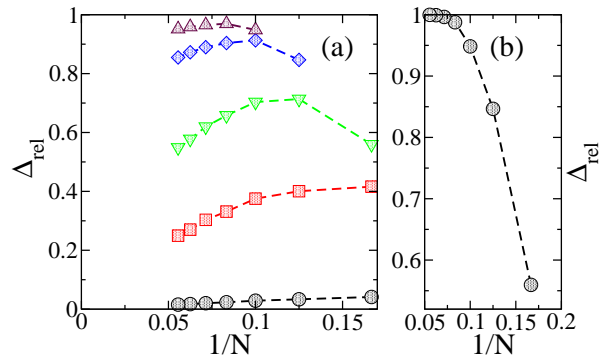


FIG. 2: (Color online) Longer-range correlations for the same quench as in Fig. 1(a). Shown is the scaling of the relative deviation between ensemble averages Δ_{rel} for (a) $|i-j|=1, 2, 3, 4, 5$ (from bottom to top) and (b) for $|i-j|=N/2$.

follows from the fact that the canonical ensemble is obtained from the diagonal one by neglecting all non-local quantities. For a finite system they do, however, contribute showing that the TDL is essential for thermalization. In the integrable case shown in the inset of Fig. 1, the canonical ensemble does not describe the equilibrated state at long times because other local conserved quantities are not taken into account [40].

Locality and observables Next, we want to study how the amount of locality of the operator itself affects its thermalization. Numerical data for $O = \langle \mathbf{S}_i \mathbf{S}_j \rangle$, which is a two-point correlation function of a fully local operator, are shown in Fig. 2. The relative deviation $\Delta_{\text{rel}} = |(\langle \mathbf{S}_i \mathbf{S}_j \rangle_{\text{diag}} - \langle \mathbf{S}_i \mathbf{S}_j \rangle_{\text{can}}) / \langle \mathbf{S}_i \mathbf{S}_j \rangle_{\text{diag}}|$ between the long-time mean (diagonal ensemble) and the canonical ensemble average becomes larger the larger the distance is and thus the less local O is, see Fig. 2(a). If we fix

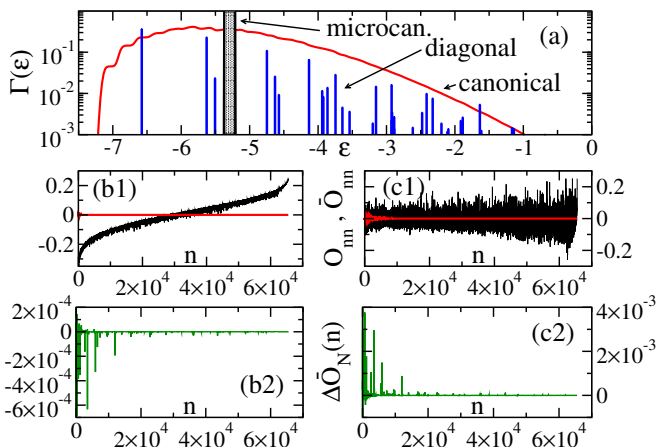


FIG. 3: (Color online) Same quench as in Fig. 1(a) for $N = 16$. Shown are: (a) the initial, microcanonical and canonical energy distribution functions, and results for $O = \mathbf{S}_i \mathbf{S}_{i+1}$ in (b) and $O = \mathbf{S}_i \mathbf{S}_{i+4}$ in (c). (b1) and (c1) show O_{nn} (black line) and \bar{O}_{nn} (red line, small fluctuations), while (b2) and (c2) show $\Delta \bar{O}_N(n)$ where the states are ordered by energy $\varepsilon_{n-1} \leq \varepsilon_n$.

the distance between the spin operators to $N/2$ as in Fig. 2(b) then the canonical ensemble average approaches zero with increasing N much faster than the long-time mean so that $\Delta_{\text{rel}} \rightarrow 1$. We conclude that the operator-dependent first term in Eq. (7), \bar{O}_{nn} , has to play a crucial role for thermalization.

Projection onto locally conserved quantities To study the role of locality of the operator in more detail we now use the splitting into a local and a non-local part introduced in Eq. (5). The initial distribution function $|c(\varepsilon_n)|^2$, and the microcanonical and canonical ones, $\Gamma_{\text{mic/can}}(\varepsilon)$, for the non-integrable quench are shown in Fig. 3(a). At least for the system sizes within the reach of exact diagonalization, the initial state distribution is not singly peaked and thus cannot be simply replaced by the microcanonical ensemble. As has been noted previously [8], O_{nn} can show monotonic behavior with comparably small fluctuations for observables related to the energy of the system, see Fig. 3(b1). However, this dependence stems entirely from the local part of the operator for which the agreement between canonical and diagonal ensemble is guaranteed by construction. If we only consider the non-local part, \bar{O}_{nn} , which according to Eq. (7) fully captures the difference between the ensembles, we see that we are left with much smaller fluctuations of order 10^{-4} around zero. O_{nn} for $\mathbf{S}_i \mathbf{S}_{i+4}$ shown in Fig. 3(c1), on the other hand, does not show a monotonic energy dependence and much larger fluctuations apparently contradicting ETH [48]. \bar{O}_{nn} , however, again shows only very small fluctuations centered around zero, see also Fig. 2(b2) of the Suppl.Mat.. Thus $\Delta \bar{O}_N(n)$, defined in Eq. (7) and shown in Fig. 3(b2) and (c2), looks qualitatively similar in the two cases with the fluctua-

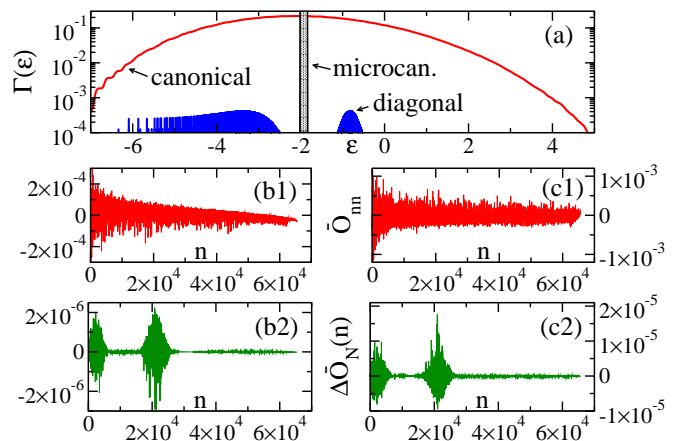


FIG. 4: (Color online) Same as Fig. 3 but for the initial state (10) with $N = 16$. In (b1) and (c1) only \bar{O}_{nn} is shown because O_{nn} remains unchanged, see Fig. 3(b1) and (c1).

tions for $\mathbf{S}_i \mathbf{S}_{i+4}$ being an order of magnitude larger.

While the initial distribution shown in Fig. 3(a) is not narrow in energy, this might still happen for larger system sizes. We thus now turn to an example where such a narrowing in energy is excluded by construction. Specifically, we consider the initial state

$$|\Psi_0\rangle = \sum_{n=1} \left[e^{-(\frac{15}{D})^2 (n - \frac{D}{30})^2} + e^{-(\frac{15}{D})^2 (n - \frac{D}{3})^2} \right] |n\rangle \quad (10)$$

where n is the index for the non-degenerate eigenenergies of $H(1, 0.2)$ ordered by magnitude. This state is one possible quantum analogue of the classical case (II) with an initial energy distribution which has two peaks, see Fig. 4(a). The microcanonical distribution now sits right between these two peaks in a region where the initial distribution has no weight. Clearly a simple replacement by the microcanonical or canonical distribution function now seems impossible. Nevertheless, the numerical data still suggest that the system thermalizes. The behavior of \bar{O}_{nn} remains, in fact, qualitatively very similar to the quench case, see Fig. 4(b1,c1). $\Delta \bar{O}_N(n)$, see Fig. 4(b2,c2), shows again small fluctuations but now in two regions corresponding to the two peaks in the initial distribution whereas in the quench case they mainly occur in the low energy part of the spectrum.

Conclusions To summarize, we have looked at the question of thermalization in closed quantum systems from the perspective of conservation laws. Contrary to a classical system two distinct kinds appear: local and non-local ones. Projecting the considered observable onto the local and non-local conserved quantities we have demonstrated that the fluctuations in the non-local part are crucial for thermalization and allow for a visualization of typicality. A restriction to initial states with a distribution sufficiently narrow in energy—which is central to ETH—is not necessary as we have demonstrated exemplarily by choosing a doubly-peaked initial distribution.

The authors acknowledge support by the Collaborative Research Centre SFB/TR49 and the Graduate School of Excellence MAINZ.

Supplementary material

The purpose of our supplementary material is twofold. On the one hand, we will provide some additional information regarding initial states which do not become narrow in energy in the thermodynamic limit, about the splitting of an observable into a local and a non-local part, as well as some technical details. Secondly, we also provide some additional data about what happens for integrable systems.

Details of the calculation

In Sec. we explain other possible setups which can lead to initial states which are not narrow in energy. In Sec. we then elaborate on some details concerning the splitting of an observable into a local and a non-local part. In Sec. we explain the coarse graining procedures used to obtain the continuous distributions. Finally, we present in Sec. some additional numerical data on how the non-local part of the considered operators scale with system size.

Setup for the initial state

An assumption when considering thermalization in closed quantum systems which is sometimes spelled out explicitly [8] or is implicitly assumed is that in the thermodynamic limit the energy distribution of the initial state is narrowly peaked at one specific energy. This indeed seems to be usually the case if a quantum quench for a Hamiltonian with local interactions is considered. However, if we have full control over the quantum system—as is the aim for trapped ions, nuclear spin systems, or cold atomic gases in order to be able, for example, to perform quantum computations—*any* initial state is possible. In the main part, we constructed one example for an initial state by hand where the distribution does not become narrow in energy in the thermodynamic limit. There are other possible ways such a state can arise: (a) One can consider a superposition of states, e.g., ground states of different Hamiltonians. In this case we also expect that in general the distribution does not peak at just one specific energy. (b) One could also consider two different thermal distributions, e.g., if parts of the system are held at different temperatures. Again, there is no reason to expect that the distribution function will peak at a single energy in the thermodynamic limit.

In the main text of the paper we have focused on pure states, the generalization to mixed states, which would be necessary for example for thermal distributions, is straightforward. In general a mixed state can be described by a density matrix

$$\rho = \sum_i p_i |\Psi_i\rangle\langle\Psi_i|, \quad (11)$$

written in terms of an orthonormal basis $|\Psi_i\rangle$. The long time average of an operator O , equivalent to Eq. (2) of the letter, becomes

$$\bar{O} = \text{Tr}[\rho O_{\text{diag}}] = \sum_{i,n} O_{nn} p_i |\langle\Psi_i|n\rangle|^2. \quad (12)$$

The $\{p_i\}$ are also assumed to be normalized, so that $\sum_i p_i = 1$. All results from the letter then apply with $\langle\Psi_0|\dots|\Psi_0\rangle \rightarrow \text{Tr}[\rho\dots]$. In particular for the projection operators we find

$$\text{Tr}[\rho P_n] = \sum_i p_i |\langle\Psi_i|n\rangle|^2. \quad (13)$$

One of the main points of our paper is that in all these cases the concept of thermalization should remain valid but that ETH is not sufficient to explain why and how the system thermalizes.

Splitting into local and non-local part

Instead, we argued that locality is the main new ingredient when thermalization in quantum systems is considered as compared to the classical case. At the heart of our arguments is a splitting of the observable into a local and a non-local part, Eq. (6) of the paper. For the local part the equivalence of the diagonal and the appropriate thermal ensemble average is then a given so that thermalization leads to a condition on the non-local part only.

Choice of inner product As in Eq. (5) of the paper we can write

$$O_{\text{diag}} = \underbrace{\frac{\langle OH \rangle}{\langle H^2 \rangle} H}_{O_{\text{loc}}} + \underbrace{\sum_{n=1}^{D-1} \frac{\langle O \bar{P}_n \rangle}{\langle \bar{P}_n^2 \rangle} \bar{P}_n}_{O_{\text{nonloc}}} \quad (14)$$

with $\langle H \bar{P}_n \rangle = 0$ and $\langle \bar{P}_n \bar{P}_m \rangle = \delta_{nm} \langle \bar{P}_n^2 \rangle$. In the paper we have chosen $\langle \dots \rangle = \langle \dots \rangle_{\text{th}} \equiv \text{Tr}\{\dots \rho_{\text{th}}\}$ as inner product in the vector space of Hermitian operators. While this is the natural choice, it is also possible to use any other proper inner product in operator space. The splitting into a local and a non-local part thus depends on the choice of the metric. This is, of course, expected since the very notion of distances requires the definition of a metric first.

Using a general inner product and projection operators \bar{P}_n which are orthogonal with respect to this metric, Eq. (7) of the paper can be written in the more general form

$$\begin{aligned} 0 &= \lim_{N \rightarrow \infty} \Delta O_N \equiv \lim_{N \rightarrow \infty} [\langle O \rangle_{\text{diag}} - \langle O \rangle_{\text{th}}] \quad (15) \\ &= \lim_{N \rightarrow \infty} \sum_{n=1}^{D-1} \underbrace{\frac{\langle O \bar{P}_n \rangle}{\langle \bar{P}_n^2 \rangle}}_{\bar{O}_{nn}} (\langle \Psi_0 | \bar{P}_n | \Psi_0 \rangle - \langle \bar{P}_n \rangle_{\text{th}}). \end{aligned}$$

We want to stress once more that ΔO_N does not depend on the choice of the inner product. It is only once we start considering the contributions on a microscopic level that this choice becomes relevant.

Energy shift Apart from the inner product there is another ‘gauge degree of freedom’ in the second line of Eq. (15). By shifting the energy, $H' = H - E_0$, the projection operators \bar{P}_n are modified because of the orthogonality condition $\langle H \bar{P}_n \rangle = 0$. The qualitative behavior of \bar{O}_{nn} is, however, not affected. A convenient, unique gauge is obtained by demanding that $\sum \bar{O}_{nn} \langle \bar{P}_n \rangle_{\text{th}} = 0$. For a general metric $\langle \dots \rangle$ this is achieved by choosing

$$E_0 = \frac{\langle OH \rangle \langle H \rangle - \langle O \rangle \langle H^2 \rangle}{\langle OH \rangle + \langle O \rangle \langle H \rangle_{\text{th}} - 2 \langle O \rangle_{\text{th}} \langle H \rangle}. \quad (16)$$

for a given Hamiltonian H and operator O . By setting $\langle \dots \rangle = \text{Tr}\{\dots \rho_{\text{th}}\}$ this expression simplifies to Eq. (7) of the paper.

Orthogonalization by a Householder reflection Once an inner product has been chosen, the projection operators have to be orthogonalized with respect to H and amongst each other, i.e., $\langle H \bar{P}_n \rangle = 0$ and $\langle \bar{P}_n \bar{P}_m \rangle = \delta_{nm} \langle \bar{P}_n^2 \rangle$. Since $\langle P_n P_m \rangle = 0$, $n \neq m$, for the regular projectors P_n independent of the inner product, the orthogonalization can be achieved by rotating $D - 1$ projectors P_n around a constant angle with respect to H . More specifically, we define the following Householder reflection R . As a first step we choose the set of normalized operators $\{\tilde{H}, \tilde{P}_1, \tilde{P}_2, \dots, \tilde{P}_{D-1}\}$ where $\tilde{H} = H / \sqrt{\langle H^2 \rangle}$ and $\tilde{P}_n = P_n / \sqrt{\langle P_n^2 \rangle}$. We now define the normalized operator

$$\tilde{U} = (\tilde{H} - \tilde{P}_D) / \sqrt{\langle (\tilde{H} - \tilde{P}_D)^2 \rangle} \quad (17)$$

so that

$$R(\tilde{H}) = \tilde{H} - 2\tilde{U} \langle \tilde{U} \tilde{H} \rangle = \tilde{P}_D. \quad (18)$$

Applying the same orthogonal transformation onto the projection operators

$$R(\tilde{P}_i) = \tilde{P}_i - 2\tilde{U} \langle \tilde{U} \tilde{P}_i \rangle = \tilde{P}_i \quad (19)$$

for $i = 1, 2, \dots, D - 1$ thus generates the required orthonormal set.

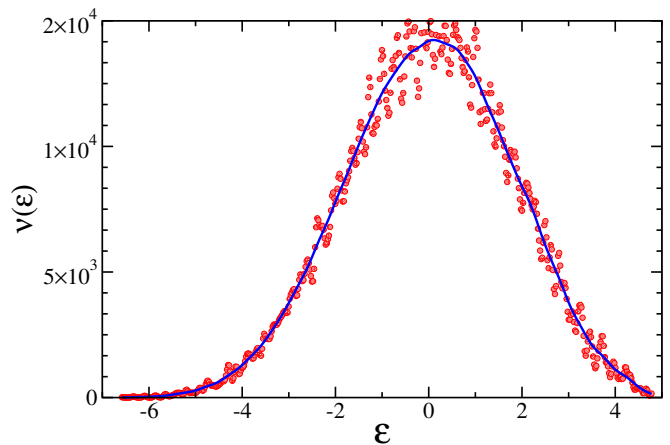


FIG. 5: (Color online) Coarse grained density of states, $\nu(\varepsilon)$, for the Hamiltonian $H(1, 0.2)$ with $N = 16$. The coarse graining width is $W = 10\delta$, where δ is the mean level spacing. Shown is the result after coarse graining (red circles), and the result after an additional running average (blue line).

Energy distributions and coarse graining

In order to plot the continuum energy distributions a coarse graining is necessary. The density of states is first made continuous by approximating

$$\nu(\varepsilon) \equiv \sum_n \delta(\varepsilon - \varepsilon_n) \approx \sum_n \chi_W(\varepsilon - \varepsilon_n), \quad (20)$$

with an envelope function:

$$\chi_W(\varepsilon) = \frac{e^{-\varepsilon^2/(2W^2)}}{\sqrt{2\pi W^2}}. \quad (21)$$

In the paper we have used $W = 10\delta$ for $N = 16$, where δ is the mean level spacing with an additional running average. The respective data are shown in Fig. 5. The same procedure is performed for the canonical ensemble. As a check that this is working correctly one must compare operator averages found with these coarse grained distributions and with the exact ones. Note that whilst a coarse graining over a wider energy range (*e.g.* $W = 50\delta$) will give the same result for the density of states as in Fig. 5, it does not give accurate results for the canonical ensemble. For the microcanonical ensemble one simply broadens the delta-function around the initial energy $E = \langle \Psi_0 | H | \Psi_0 \rangle$,

$$\Gamma_{\text{mic}}(\varepsilon) \approx \theta(\varepsilon - E + W/2) - \theta(\varepsilon - E - W/2), \quad (22)$$

where $\theta(\varepsilon)$ is the Heaviside function.

In principle one could also attempt this procedure on the diagonal ensemble. However for the system sizes we are able to consider we find that it is not possible to smoothen the diagonal ensemble and, at the same time, retain accurate averages for physical quantities.

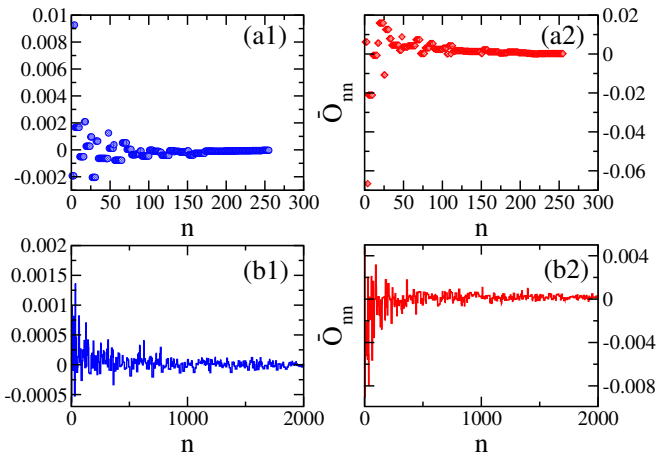


FIG. 6: (Color online) Quench with $|\Psi_0(5, 0.2)\rangle$ and $H(1, 0.2)$. Shown is a comparison of \bar{O}_{nn} for different system sizes: (a) $N = 8$ and (b) $N = 16$. (a1) and (b1) are for $O = \mathbf{S}_i \mathbf{S}_{i+1}$. (a2) and (b2) are for $O = \mathbf{S}_i \mathbf{S}_{i+4}$. A reduction in the overall scale of the fluctuation is clearly visible for increasing system size. Note that only part of the spectrum is shown in (b1) and (b2).

Scaling of non-local fluctuations

Here we will provide some additional information on how the non-local fluctuations scale with system size for the quench with $|\Psi_0(5, 0.2)\rangle$ and $H(1, 0.2)$ considered in the paper. In Fig. 6 we plot \bar{O}_{nn} for different system sizes. From $N = 8$ to $N = 16$ a reduction in the scale of the fluctuations of an order of magnitude is visible. In order for ΔO_N to vanish in the thermodynamic limit it is in general necessary that a macroscopic number of contributions is picked, i.e., $\langle \Psi_0 | \hat{P}_n | \Psi_0 \rangle \neq 0$ for a macroscopic number of states. This condition is necessary but not sufficient for a typical initial state.

The integrable case

Non-equilibrium dynamics in integrable systems and the question of the appropriate statistical ensemble to describe the long-time limit has been intensely studied in recent years.[21, 40–43] In our paper we only briefly touched upon this issue by explaining how the splitting into a local and a non-local part can be generalized to the integrable case. While for non-interacting systems the additional local conservation laws simply become the occupation numbers of the diagonal modes they are quite complicated in the interacting case [28] and a detailed study is beyond the scope of this letter. Here we simply want to look for indications of integrability when taking only the Hamiltonian itself into the local part, as in Eq. (5) of the paper, thus ignoring all other locally conserved quantities. In Fig. 7 we present the same data as in Fig. 2 of the paper but for the integrable quench

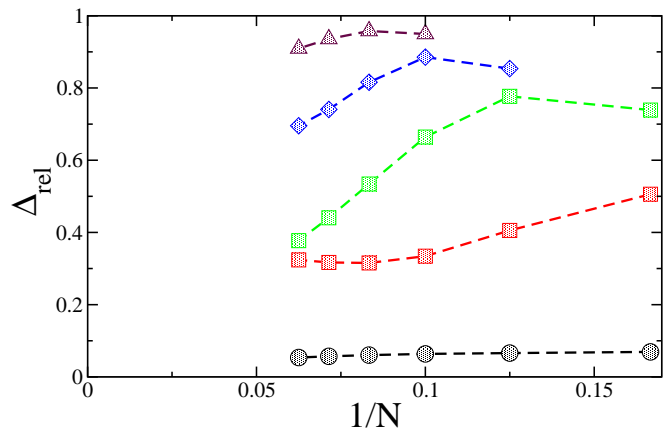


FIG. 7: (Color online) Longer-range correlations for the integrable quench. Shown is the scaling of the relative deviation between ensemble averages Δ_{rel} for $|i - j| = 1, 2, 3, 4, 5$ (from bottom to top).

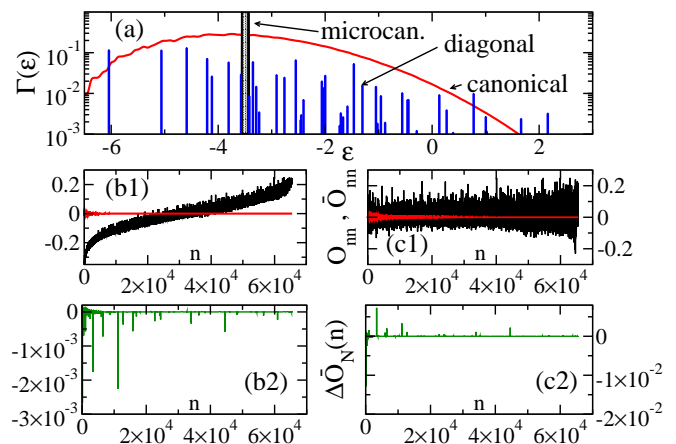


FIG. 8: (Color online) Integrable quench for $N = 16$. Shown are: (a) the initial, microcanonical and canonical energy distribution functions, and O_{nn} (black line) and \bar{O}_{nn} (red line, small fluctuations) $[\Delta O_N(n)]$ for $O = \mathbf{S}_i \mathbf{S}_{i+1}$ in (b1) [(b2)] and similarly for $O = \mathbf{S}_i \mathbf{S}_{i+4}$ in (c1) [(c2)] where the states are ordered by energy $\epsilon_{n-1} \leq \epsilon_n$.

with $|\Psi_0(5, 0)\rangle$ and $H(1/2, 0)$. The scaling behavior is now quite different. Δ_{rel} for the correlation function $\langle \mathbf{S}_i \mathbf{S}_{i+2} \rangle$, in particular, shows an upturn for the largest system sizes indicating that the canonical ensemble does not describe the system at long times. To understand the scaling of the different correlation functions in more detail, an analysis of the overlap of each operator O with the local conserved quantities would be required.

Finally, we present in Fig. 8 the analogue of Fig. 3 of the paper for the integrable case. One of the obvious differences is that the fluctuations in O_{nn} for the case $O = \mathbf{S}_i \mathbf{S}_{i+1}$ are substantially larger than in the non-integrable case, see Fig. 8(b1). Furthermore, Fig. 8(b2) shows that the corresponding fluctuations in $\Delta O_N(n)$ are an order of magnitude larger than in the non-integrable

case with substantial contributions even high up in the spectrum. This could possibly be related to the different energy level distributions. While level repulsion leads to a Wigner-Dyson distribution for a generic model, each state in an integrable model is uniquely characterized by the quantum numbers of the local conserved quantities so that states can cross. This leads to a Poissonian distribution and might be responsible for the different structure of fluctuations in Fig. 8(b2) and (c2). The fact that we are missing local conservation laws when using the canonical ensemble for an integrable system would, of course, be immediately obvious if we choose one of the additional local conserved operators as our observable whose expectation value would be time independent and thus characterized by the initial microstate.

-
- [1] L. D. Landau and E. M. Lifshitz, *Statistical Physics* (Butterworth-Heinemann, Oxford, 1980).
- [2] G. D. Birkhoff, Proc. Natl. Ac. Sci. **17**, 656 (1931).
- [3] J. von Neumann, Proc. Natl. Ac. Sci. **18**, 70 (1932).
- [4] G. Morandi, F. Napoli, and E. Ercolessi, *Statistical Mechanics: An intermediate course* (World Scientific, Singapore, 2001).
- [5] M. Tabor, *Chaos and integrability in nonlinear dynamics: an introduction* (Wiley, New York, 1989).
- [6] J. M. Deutsch, Phys. Rev. A **43**, 2046 (1991).
- [7] M. Srednicki, Phys. Rev. E **50**, 888 (1994).
- [8] M. Rigol, V. Dunjko, and M. Olshanii, Nature **452**, 854 (2008).
- [9] P. Calabrese, F. H. L. Essler, and M. Fagotti, Phys. Rev. Lett. **106**, 227203 (2011).
- [10] N. Sedlmayr, J. Ren, F. Gebhard, and J. Sirker, Phys. Rev. Lett. **110**, 100406 (2013).
- [11] F. Gebhard, K. zu Münster, J. Ren, N. Sedlmayr, J. Sirker, and B. Ziebarth, Ann. Phys. (Berlin) **524**, 286 (2012).
- [12] T. Kinoshita, T. Wenger, and D. S. Weiss, Nature **440**, 900 (2006).
- [13] S. Trotzky, Y.-A. Chen, A. Flesch, I. P. McCulloch, U. Schollwöck, J. Eisert, and I. Bloch, Nat. Phys. **8**, 325 (2012).
- [14] N. Strohmaier, D. Greif, R. Jördens, L. Tarruell, H. Moritz, T. Esslinger, R. Sensarma, D. Pekker, E. Altman, and E. Demler, Phys. Rev. Lett. **104**, 080401 (2010).
- [15] S. Hofferberth, I. Lesanovsky, B. Fischer, T. Schumm, and J. Schmiedmayer, Nature **449**, 324 (2007).
- [16] T. Enss and J. Sirker, New J. Phys. **14**, 023008 (2012).
- [17] S. R. Manmana, S. Wessel, R. M. Noack, and A. Muramatsu, Phys. Rev. Lett. **98**, 210405 (2007).
- [18] M. Rigol, A. Muramatsu, and M. Olshanii, Phys. Rev. A **74**, 053616 (2006).
- [19] G. Biroli, C. Kollath, and A. M. Läuchli, Phys. Rev. Lett. **105**, 250401 (2010).
- [20] C. Kollath, A. M. Läuchli, and E. Altman, Phys. Rev. Lett. **98**, 180601 (2007).
- [21] M. Rigol, V. Dunjko, V. Yurovsky, and M. Olshanii, Phys. Rev. Lett. **98**, 050405 (2007).
- [22] E. Canovi, D. Rossini, R. Fazio, G. E. Santoro, and A. Silva, Phys. Rev. B **83**, 094431 (2011).
- [23] M. A. Cazalilla, Phys. Rev. Lett. **97**, 156403 (2006).
- [24] L. F. Santos, A. Polkovnikov, and M. Rigol, Phys. Rev. Lett. **107**, 040601 (2011).
- [25] T. N. Ikeda, Y. Watanabe, and M. Ueda, Phys. Rev. E **84**, 021130 (2011).
- [26] J. von Neumann, Z. Phys. **57**, 30 (1929); Eur. Phys. J. H **35**, 201 (2010).
- [27] F. H. L. Essler, H. Frahm, F. Göhmann, A. Klümper, and V. E. Korepin, *The One-Dimensional Hubbard model* (Cambridge University Press, Cambridge, 2005).
- [28] M. Grabowski and P. Mathieu, Ann. Phys. **243**, 299 (1995).
- [29] G. Roux, Phys. Rev. A **81**, 053604 (2010); Phys. Rev. A **82**, 037602 (2010).
- [30] T. Prosen, Phys. Rev. Lett. **106**, 217206 (2011).
- [31] X. Zotos, F. Naef, and P. Prelovšek, Phys. Rev. B **55**, 11029 (1997).
- [32] A. Rosch and N. Andrei, Phys. Rev. Lett. **85**, 1092 (2000).
- [33] J. Sirker, R. G. Pereira, and I. Affleck, Phys. Rev. Lett. **103**, 216602 (2009).
- [34] J. Sirker, R. G. Pereira, and I. Affleck, Phys. Rev. B **83**, 035115 (2011).
- [35] P. Mazur, Physica **43**, 533 (1969).
- [36] M. Suzuki, Physica **51**, 277 (1971).
- [37] N. P. Konstantinidis, Phys. Rev. B **72**, 064453 (2005).
- [38] P. Barmettler, M. Punk, V. Gritsev, E. Demler, and E. Altman, Phys. Rev. Lett. **102**, 130603 (2009).
- [39] P. Barmettler, M. Punk, V. Gritsev, E. Demler, and E. Altman, New J. Phys. **12**, 055017 (2010).
- [40] M. Fagotti and F. H. L. Essler, arXiv:1302.6944 (2013).
- [41] L. F. Santos and M. Rigol, Phys. Rev. E **81**, 036206 (2010).
- [42] L. F. Santos and M. Rigol, Phys. Rev. E **82**, 031130 (2010).
- [43] J.-S. Caux and R. M. Konik, Phys. Rev. Lett. **109**, 175301 (2012).
- [44] For a system which has a local representation in momentum space the same approach can be used where locality in momentum space is defined accordingly.
- [45] We work here directly with the canonical ensemble to circumvent the difficulties of coarse graining when defining a microcanonical ensemble, see also the Suppl. Mat..
- [46] Any metric in operator space can, in principle, be used here with the one induced by ρ_{th} being the natural choice, see also the Suppl. Mat..
- [47] This can be achieved by a Householder reflection, see the Suppl. Mat. for details.
- [48] Defining an $O(\varepsilon)$ in the TDL by averaging over a small energy window will, of course, lead to a continuous function.